ELSEVIER

Biochimica et Biophysica Acta 1412 (1999) 273–281

BIOCHIMICA ET BIOPHYSICA ACTA

BBA

www.elsevier.com/locate/bba

Determination of Q_A-content in bacterial reaction centers: an indispensable requirement for quantifying B-branch charge separation

A. Ogrodnik *, P. Müller, G. Hartwich, M.E. Michel-Beyerle

Institut für Physikalische und Theoretische Chemie, TU München, Lichtenbergstr. 4, D-85747 Garching, Germany

Received 15 February 1999; received in revised form 17 June 1999; accepted 17 June 1999

Abstract

We have been able to determine the occupancy of the quinone site at the A-branch (Q_A) of a reaction center preparation with an accuracy of 2%. This is achieved by accumulating the $P^+Q_A^-$ state after multiple actinic excitation and monitoring the extent of the 30 ms ground state bleaching. This bleaching is corrected for deviations from complete saturation due to competing charge separation to the B-branch. On the other hand, knowledge of the Q_A content is indispensable for determining the yield of B-branch charge separation from nanosecond transients associated with the recombination of $P^+H_B^-$, which have to be corrected for the nanosecond signal originating from $P^+H_A^-$ of RCs having lost Q_A.

Keywords: $P^+Q_A^-$ recombination; Ubichinone; Saturation spectroscopy; Quantum yield; B-branch charge separation; $P^+H_B^-$; (*Rhodobacter sphaeroides*)

1. Introduction

Though the crystal structure analysis [1–5] of bacterial reaction centers (RCs) reveals a 2-fold symmetry with two branches of cofactors lining up to the primary donor and offering themselves as electron acceptors, electron transport proceeds exclusively along one of these acceptor branches in native RCs [6–12]. Starting from the donor P, a bacteriochlorophyll dimer, charge separation carries on to a bacteriochlorophyll monomer (B_A), a bacteriopheophytin (H_A) and a quinone (Q_A) in subsequent electron transfer steps at the so called A-branch. With the exception of the very final ET step, in which Q_B is reduced, the corresponding cofactors of the B-branch are not involved in functioning native RCs, because the primary step to $P^+B_B^-$ or $P^+H_B^-$ is slow.

Formation of $P^+B_B^-$ or $P^+H_B^-$ can be fostered by slowing down the primary charge separation step on the A-branch. It has been shown, that the decay of $^1P^*$ can be slowed down by a factor of $\sim$25 at low temperatures when the native bacteriochlorophyll at the B_A site is exchanged against 3-vinyl-13^2-OH-bacteriochlorophyll (vinyl$_A$-RCs), because the increase of its in vitro reduction potential by $\sim$1000 cm^{-1} leads to an activation barrier for charge separation [14,15]. This allows to quantitatively study this reaction and thus to elucidate the reason for the kinetic asymmetry.

Spectroscopic access to the ratio of A- and B-

Abbreviations: RC, reaction center; P, primary donor; $H_{A,B}$, $B_{A,B}$, and $Q_{A,B}$, bacteriopheophytin, monomeric bacteriochlorophyll and ubiquinone at their binding sites in the reaction center

* Corresponding author. Fax: +49-89-289-13026;
E-mail: alexander.ogrodnik@ch.tum.de

0005-2728/99/$ – see front matter
PII: S0005-2728(99)00070-5

branch charge separation is obstructed by the fact that the A- and B-branch cofactors are difficult to discriminate. Merely the Q_x-absorption bands of H_A (546 nm) and H_B (533 nm) are split at low temperature in *Rhodobacter sphaeroides* [13] and formation of $P^+H_A^-$ is accompanied by selective bleaching of H_A. Quantification of low yields of $P^+H_B^-$, however, is hindered by electrochromic shifts and background transient absorptions. RCs of *Chloroflexus aurantiacus* give an example of how misleading small spectral features can be: in addition to the bleaching of H_A (at 540 nm) a distinct blue shoulder has been observed, suggesting a significant amount of $P^+H_B^-$ formation. This conception had to be dismissed, since decay kinetics of this shoulder changes from 15 ns in absence of Q_A to $\sim$300 ps on reconstitution of Q_A in the same way as the H_A signal [8]. In vinyl$_A$-RCs, likewise a transient bleaching around 530 nm has been observed. In this case, however, the bleaching survives for nanoseconds even in presence of Q_A, suggesting that it indeed reflects formation and decay of $P^+H_B^-$ [14,15].

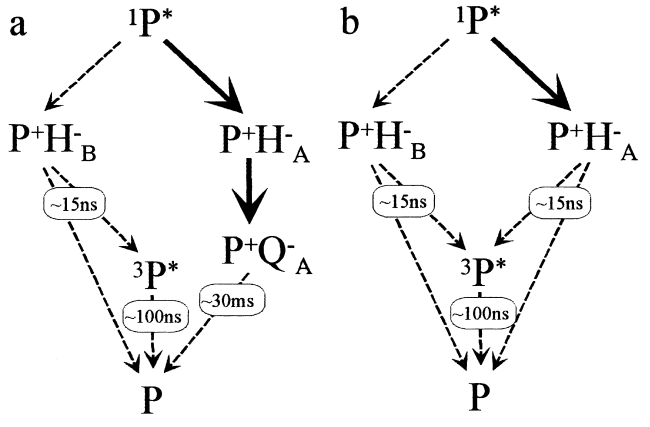

While it is risky to prove asymmetric charge separation by spectral discrimination, it is easy to introduce a preparational asymmetry having only Q_A present as an electron acceptor, but not Q_B. According to the simplified reaction scheme (1a), such an assay promises a clear discrimination between A- and B-branch charge separation based on the differing decay characteristics expected for $P^+H_B^-$ as compared to that of $P^+Q_A^-$. $P^+Q_A^-$ recombines to the ground state in 30 ms (at 80 K), while we expect a recombination of $P^+H_B^-$ on the nanosecond timescale. In both cases the bleaching of the ground state will recover and can conveniently be monitored at 860–890 nm, without significant spectral contributions from other transient species. In the G(M201)D/L(M212)H double mutant of *Rb. capsulatus* recombination of $P^+H_B^-$ was observed on the timescale of tens of nanoseconds [9]. Similar signals have been observed when the native bacteriochlorophyll at the B_A site of wild-type RCs is exchanged against 3-vinyl-13^2-OH-bacteriochlorophyll (vinyl$_A$-RCs) [14,15].

An alternative approach to infer on B-branch charge separation from the observed nanosecond kinetics has been applied to reaction centers of *Rhodopseudomonas viridis*, in which the state $PH_A^-Q_A^-$ can be photo-accumulated via efficient reduction of P^+ by the bound cytochromes. In this case $P^+H_A^-Q_A^-$ can no longer be formed and at first sight one expects no nanosecond signal from $P^+H_A^-$ recombination. It was shown, however, that a transient with a lifetime of 20–30 ns still remains, which is thought to reflect $P^+H_B^-$ recombination to the special pair triplet state $^3P^*$ [16]. While there is no doubt that $P^+H_B^-$ is formed in such a situation, quantitative conclusions have to be dealt with caution, since the recombination pathways are rather complex. Because of the presence of $H_A^-Q_A^-$ we have the overall state $H_B^-P^+H_A^-Q_A^-$, in which the two radical pairs $P^+H_B^-$ and $P^+H_A^-$ are competing with one another for recombination. The matter is further complicated by the differences in spin correlation of these two pairs. Last but not least, the charge separation dynamics on the B-branch operating in such an assay might be considerably altered by the presence of the two excess electrons on H_A and Q_A.

Thus, determination of the yield of $P^+H_B^-$ formation from the amplitude of the nanosecond recovery of the ground state absorption of P in the 865 nm band in presence of Q_A seems to be a safe and simple way of quantifying B-branch charge separation in modified reaction centers. Such an assay requires that there are no additional contributions to the nanosecond signal from reaction centers which have lost Q_A and which exhibit recombination of $P^+H_A^-$ according to scheme 1b. Indeed, it cannot be excluded that Q_A reconstitutes much less efficiently in modified RCs with potential B-branch charge separation than in wild-type. In wild-type RCs it is well known that $P^+H_A^-$ partly recombines to the ground state P and partly to the triplet state of the primary

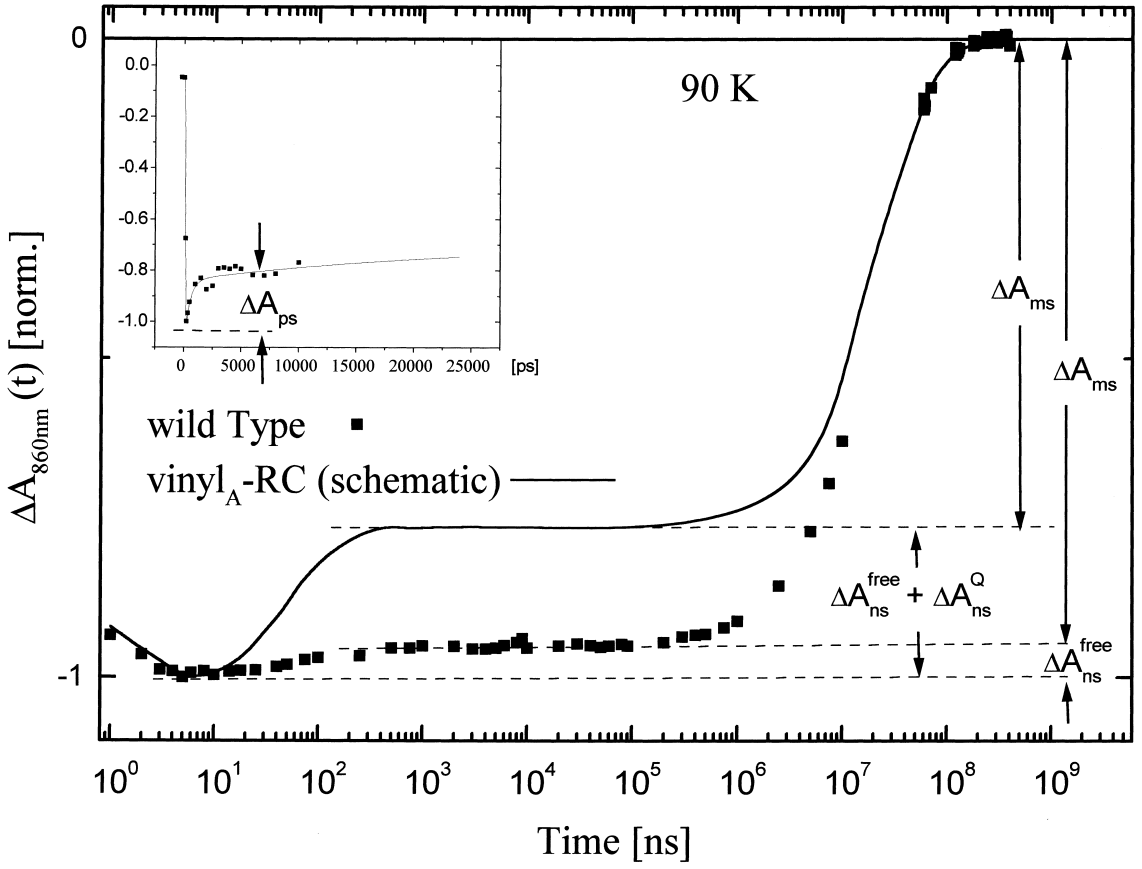

Fig. 1. Nanosecond and millisecond recovery of the P ground state absorption detected at 860 nm. ΔA_{ns} and ΔA_0 are indicated: ΔA_{ns}^{free} consists only of contributions from $P^+H_A^-$ of Q_A-free RCs in a wild type sample. In vinyl$_A$-RCs $P^+H_B^-$ decay should lead to ΔA_{ns}^{Q} of the Q-containing part of the sample and give an additional contribution to ΔA_{ns}^{free} as indicated schematically. Here we have chosen a wild type sample with $\Delta A_{ns}/\Delta A_0 = \alpha = 5\%$ (Eq. 2) for illustration. For the determination of ε_r in saturation measurements (Figs. 3 and 4) a wild-type sample with $\alpha = 1\%$ was chosen (not shown). For vinyl$_A$-RCs $\alpha = 23.6\%$ is obtained in [15]. The inset shows the picosecond recovery of vinyl$_A$-RCs due to internal conversion with an amplitude $\Delta A_{ps} \propto (c_Q + c_{free}) \cdot Y_{IC}$ yielding $Y_{IC} = 25\%$ [35].

donor $^3P^*$ within 15 ns [17–22]. The triplet channel leads to ground state recovery when energy transfer carries on to the carotinoid within 90 ns [23–27]. As an illustration, the ns- and ms-recovery of the ground state absorption resulting from $P^+H_A^-$ and from $P^+Q_A^-$ recombination of wild-type RCs, of which 5% have lost Q_A, are shown in Fig. 1. Such kinetic features have earlier been utilized for precise determination of the Q_A content of RCs [28]. This method becomes invalid, however, in presence of B-branch charge separation, since discrimination between $P^+H_A^-$ and $P^+H_B^-$ recombination is not possible. Therefore we need a complementary method for determining the Q_A content with high precision, which is immune against signals from the B-branch. In this paper we develop such a method based on quantifying the ms-time-resolved bleaching of the 865 nm band after accumulation of $P^+Q_A^-$ under well-defined saturating conditions. This method will be applied to determine the Q_A content of vinyl$_A$-RCs, giving a basis for the quantification of B-branch charge separation.

2. Materials and methods

2.1. Determination of $P^+H_B^-$ yield from nanosecond recovery of the ground state absorption

In [15] the quantum yield Y_B of $P^+H_B^-$ formation

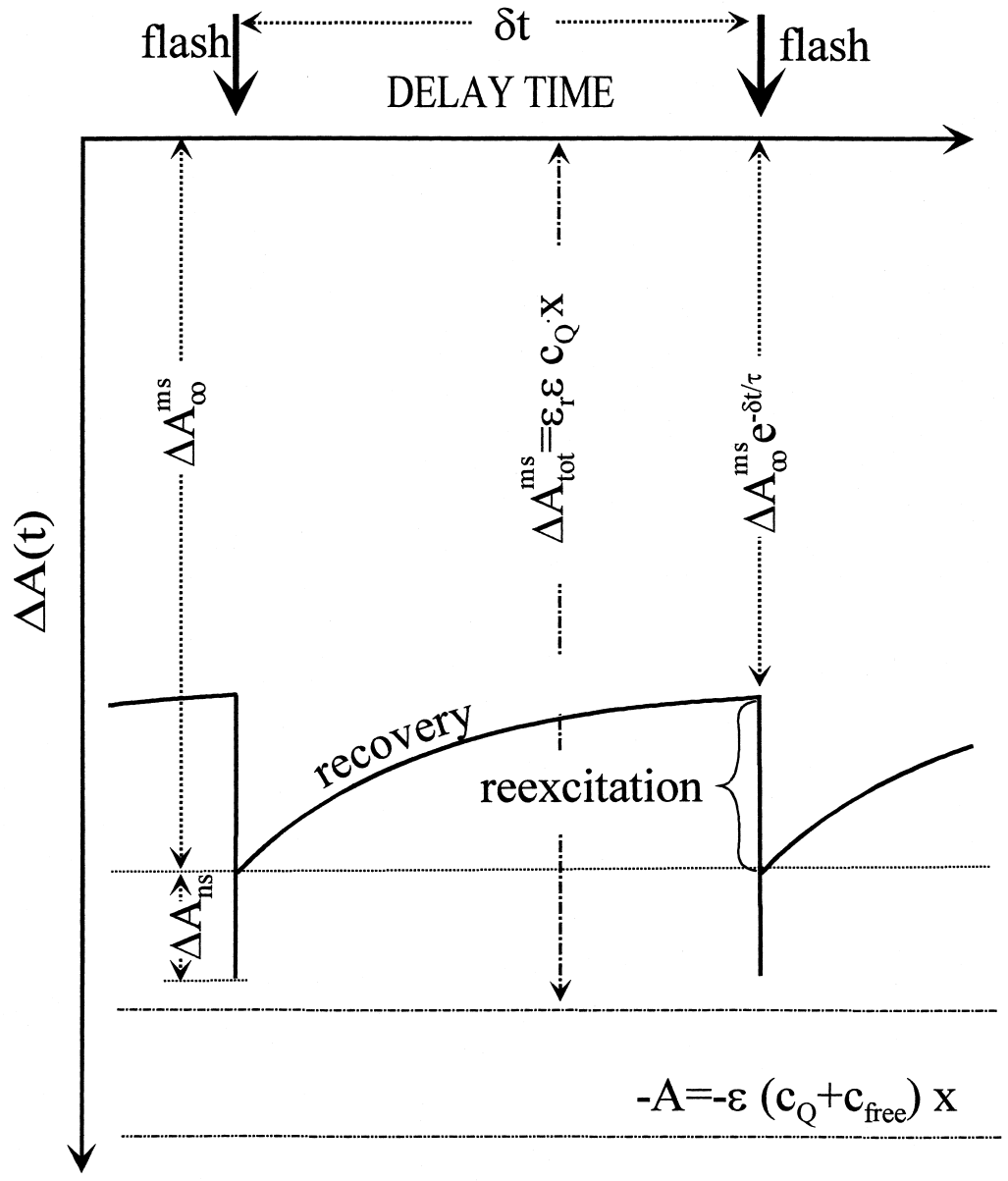

Fig. 2. Schematic recovery of the P ground state absorption after repetitive saturating excitation.

is derived from the nanosecond recovery of the ground state absorption of P in vinyl$_A$-RCs. In doing so no effort is made to resolve the bi-phasic recovery of the ground state due to (i) direct recombination via the singlet recombination channel in $\approx$15 ns and (ii) energy transfer from ^{3}P* to the carotinoid within 90 ns as indicated in scheme 1a. Furthermore, we do not try to discriminate between the recombination pattern of $P^+H_B^-$ and that of $P^+H_A^-$, since a priori we do not know that of $P^+H_B^-$. In fact recombination of both radical pairs is expected to be similar, so that it would be very difficult to discriminate between the two contributions on grounds of kinetic differences. In this context we merely have to assume that all the recovery components associated with $P^+H_A^-$ and $P^+H_B^-$ recombination occur on the timescale of a few nanoseconds to hundreds of nanoseconds. On such terms the sum of their amplitudes ΔA_{ns} can easily be distinguished experimentally from the millisecond recovery due to the recombination of $P^+Q_A^-$ and the unresolved picosecond recovery due to internal conversion (Fig. 1). For extraction of Y_B from

such nanosecond data one has to account for the magnitude of the $P^+H_A^-$ signal, which will be derived from the explicit knowledge of the Q_A content (Eq. 2). We define the relative concentration of the Q-free RCs $\gamma_f = c_{free}/(c_Q+c_{free})$ and will show in the following that γ_f can be gained from additional experimental data.

The Q_A-containing fraction of RCs (with a concentration c_Q) will contribute to ΔA_{ns} with an overall amplitude $\Delta A_{ns}^{Q} \propto c_Q \bullet Y_B$, resulting from recombination of $P^+H_B^-$ only, while it produces a millisecond amplitude, $\Delta A_{ms}^{Q} \propto c_Q \bullet Y_Q$, due to recombination of $P^+Q_A^-$ (quantum yield Y_Q). Unfortunately both $P^+H_A^-$ and $P^+H_B^-$ will contribute to the ns-absorption change of any Q_A-free RCs (with a concentration c_{free}). The corresponding overall amplitude is proportional to all RCs which have not suffered internal conversion (quantum yield Y_{IC}): $\Delta A_{ns}^{free} \propto c_{free} \bullet (1-Y_{IC})$. These RCs do not make a millisecond signal.

With the knowledge of γ_f we can account for the two contributions to the nanosecond signal $\Delta A_{ns} = \Delta A_{ns}^{Q} + \Delta A_{ns}^{free}$ (compare Fig. 1) and derive the yield for B-branch charge separation from the relative amount of the experimentally determined overall nanosecond recovery $\alpha = \Delta A_{ns}/(\Delta A_{ns}+\Delta A_{ms})$:

$$Y_B = (\alpha - \gamma_f) \bullet \frac{1-Y_{IC}}{1-\gamma_f} \quad (2)$$

In case there were no Q_A-free RCs present ($\gamma_f = 0$), α would directly give the following ratio of charge separation to the B- and A-branch: $Y_B/(Y_A+Y_B) = \alpha$. In absence of B-branch charge separation ($Y_B = 0$), on the other hand, α represents the Q_A content according to $\gamma_f = \alpha$. In practice, however, we need independent knowledge on γ_f.

2.2. Determination of the Q_A content from the millisecond bleaching of the ground state at saturating conditions

It is the intention of this paper to derive the Q_A content of a sample by accumulating all the Q_A-containing reaction centers in the state $P^+Q_A^-$ under saturating actinic conditions. The ground state absorption of all these reaction centers will bleach for milliseconds, while the Q_A depleted reaction centers remain unbleached. A comparison with the total absorption of the sample thus gives information on the Q_A content. We will show, however, that in presence of B-branch charge separation multiple actinic pulses are necessary to obtain a maximum concentration of $P^+Q_A^-$. It will be shown elsewhere that alternatively accumulation of $P^+Q_A^-$ just prior to a nanosecond measurement can be utilized to determine ΔA_{ns}^{Q} directly.

In a classical saturation experiment with a single actinic pulse the yield Y of photochemical products is derived from the number of turnovers Y necessary to deplete the ground state by monitoring the concentration of the educt (or one of the products) as a function of the actinic energy E. This signal will be proportional to the saturation function [29,30]:

$$S(E) = 1 - e^{-\sigma \bullet N(E) \bullet Y} \quad (3)$$

with σ being the cross-section of the ground state absorption, and N the photon density. Such an experiment can only discriminate between reaction channels leading to ground state recovery within the duration of the actinic pulse (total yield $1-Y$) and reactions forming photoproducts with longer lifetime (yield Y). It cannot distinguish between different such photoproducts, however. In our situation this means that Y accounts for all photoproducts living longer than $\sim$5 ns, including both $P^+Q_A^-$ *and* $P^+H_B^-$ in Q_A-containing RCs. Therefore the observed energy dependence will scale with $Y = Y_Q + Y_B = 1 - Y_{IC}$. At full saturation the single pulse yield of $P^+Q_A^-$ will be $Y_Q/Y = Y_Q/(1-Y_{IC})$. Considering that Q_A-free RCs cannot form $P^+Q_A^-$, the amplitude of the millisecond bleaching in a mixed sample (with total steady-state absorption A) is:

$$\Delta A_1^{ms}(E)/A = S(E) \bullet \varepsilon_r \bullet (1-\gamma_f) \bullet \left(1 - \frac{Y_B}{1-Y_{IC}}\right) \quad (4)$$

As for the nanosecond experiments, Y_B and γ_f cannot be derived separately.

To overcome this dilemma one would want to accumulate as many of the Q_A-containing RCs in the state $P^+Q_A^-$ as possible. This can be achieved by waiting until $P^+H_B^-$ has decayed (>100 ns) and then repeatedly exciting the sample within the lifetime of $P^+Q_A^-$. If the repetition interval (δt) of the actinic pulses is not short enough compared to the lifetime of $P^+Q_A^-$, accumulation remains incomplete, but can be quantified as follows. After a sufficient

amount of actinic pulses ($\rightarrow$'∞') the response of the system to the actinic pulses recurs in a quasi-stationary sense (schematically shown in Fig. 2): The *decay* of the maximum bleaching ΔA_{∞}^{ms} after each actinic pulse is equal to the *reexcitation* by the next actinic pulse:

$$\Delta A_{\infty}^{ms} \bullet \left(1 - e^{\frac{-\delta t}{\tau_4}}\right) = \left[\Delta A_{tot}^{ms} - \Delta A_{\infty}^{ms} \bullet e^{\frac{-\delta t}{\tau_4}}\right] \bullet S \bullet \frac{Y_Q}{1 - Y_{IC}} \quad (5)$$

On the left side the amount of recovery is given. On the right side the reexcitation amplitude is proportional to the ground state population just before reexcitation occurs and is given by the *total* concentration c_Q (the corresponding absorption change is $\Delta A_{tot}^{ms} \propto \varepsilon_r \bullet \varepsilon \bullet c_Q$) minus the $P^+Q_A^-$ concentration remaining prior to reexcitation (the corresponding bleaching is just the signal measured prior to the next actinic pulse: $\Delta A_{\infty}^{ms} \bullet e - \delta t/\tau$). ε is the extinction coefficient of the ground state absorption, ε_r the relative extent to which this band is bleached on $P^+Q_A^-$ formation. The value of ε_r will be borne out as a by-product from the experimental saturation data. As in Eq. 4, S determines the degree of reexcitation and $Y_Q/(1-Y_{IC})$ reminds us that only part of the reexcited RCs form $P^+Q_A^-$. Eq. 5 defines the relation between ΔA_{∞}^{ms}, which can be measured, and ΔA_{tot}^{ms}, which is proportional to c_Q. We relate ΔA_{tot}^{ms} to the total absorption of the sample and obtain for the concentration of Q_A-free RCs using $\beta = \Delta A_{\infty}^{ms}/(\varepsilon_r \bullet A)$:

$$\gamma_f = 1 - \frac{\Delta A_{tot}^{ms}}{\varepsilon_r \bullet A} =$$

$$1 - \beta \bullet \left\{ \frac{1 - Y_{IC}}{S(E) \bullet Y_Q} \bullet \left(1 - e^{\frac{-\delta t}{\tau}}\right) + e^{\frac{-\delta t}{\tau}} \right\} \quad (6)$$

As one would expect, ΔA_{∞}^{ms} approaches ΔA_{tot}^{ms} at high laser repetition rates ($\delta t \rightarrow 0$) and we get $\gamma_f \rightarrow 1-\beta$. Since we cannot accommodate this condition in our experiment, we could derive both γ_f and Y_B ($= 1 - Y_{IC} - Y_Q$) by measuring β at two different values of δt. Alternatively, a comparison of ΔA_{∞}^{ms} and ΔA_1^{ms} would give access to γ_f and Y_B according to Eqs. 4 and 5. Here we resort to the ns-absorption data α. Inserting Eq. 2 into Eq. 6 we obtain:

$$\gamma_f = 1 - \beta \bullet \frac{S \bullet (1-\alpha) \bullet e^{\frac{-\delta t}{\tau}}}{S \bullet (1-\alpha) - \beta \bullet \left(1 - e^{\frac{-\delta t}{\tau}}\right)} \quad (7)$$

This value can now be used to determine Y_B correctly from Eq. 2.

2.3. Sample preparation and experimental setup

RCs from *Rb. sphaeroides* R26 were prepared by standard methods [31]. Derivation of 3-vinyl-13^2-OH-bacteriochlorophyll [32] and its substitution at the B_A site by thermal exchange is described elsewhere [33,34]. The Q_A-content in native RCs used for saturation measurements was determined to be 98% according to the method in Ref. [28].

Transient absorption of P was measured in the peak of the band at 891 nm at 90 K. Saturation experiments were performed on a dedicated ms-absorption spectrometer using an excimer pumped dye laser for excitation (891 nm) and a monochromatic cw-light (tungsten lamp, monochromator) for probing the transient absorption at the same wavelength. Special care was taken to excite the sample under completely isotropic conditions in all three dimensions (including transition moments parallel to the propagation axis of the probe beam). Such precautions are of particular value in saturation experiments. For determining $\Delta A_{\infty}^{ms}/A$, the steady-state absorbance A was determined directly in situ with the ms-spectrometer ensuring identical conditions.

3. Results and discussion

In Fig. 3 the initial amplitude of the millisecond signal as a function of the energy of a single excitation pulse is shown. While in wild-type RCs losses can be neglected [29,30], one can see that *S(E)* for vinyl$_A$-RCs saturates at higher energies. Fitting the data to Eqs. 3 and 4 (see Fig. 3 for details) we obtain $Y_{IC} = (24.4 \pm 1)\%$. Such losses have been reported earlier [35] and have been attributed to internal con-

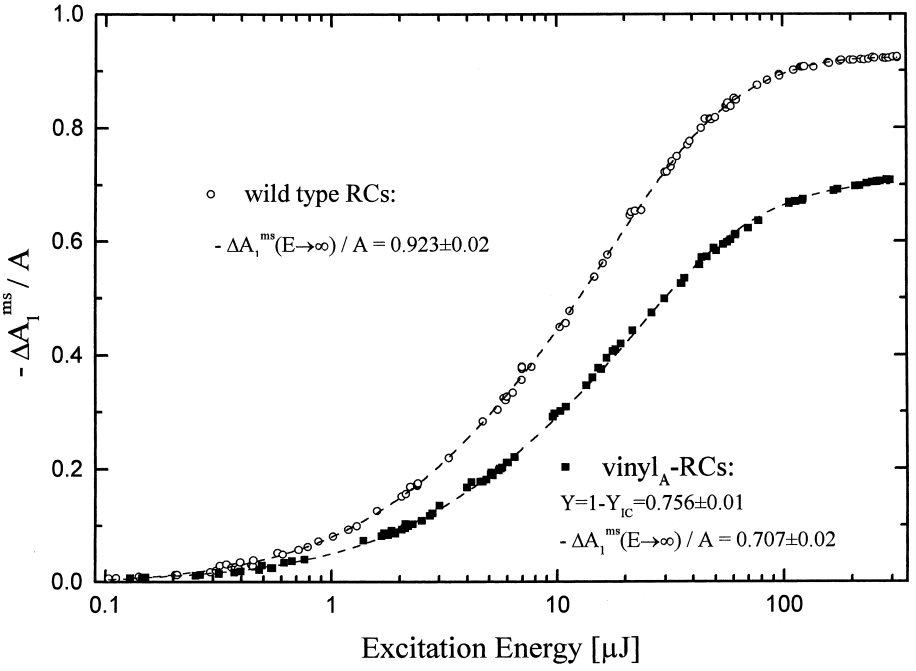

Fig. 3. The amplitude of the millisecond absorption transient as a function of the energy E of a single excitation pulse, which according to Eq. 4 reflects the saturation function $S(E)$: $\Delta A_1^{ms}(E)/A = -\Delta A_1^{ms}(E \rightarrow \infty)/A \bullet S(E)$. Excitation and detection in the maximum of the band at $\lambda = 891$ nm at $T = 90$ K. Deviations from Eq. 3 can be reduced considerably when provision is made for complete polarisational isotropy (see Section 2). The remaining small deviations may result from: (i) the lifetime of $^1P^*$ in vinyl$_A$-RCs is not short as compared to the excitation pulse length, (ii) samples are not thin enough for homogeneous excitation (iii) the 891 nm band is inhomogeneous leading to a distribution of σ. We empirically fit data according to $S(E) = 1 - \sum_{i=1}^{3} a_i \bullet \exp(-(E \bullet Y)/e_i)$ with $(\sum_i a_i = 1)$ and using $Y \approx 1$ for wild-type RCs we obtain $e_1 = 2.47$ μJ, $a_1 = 14.8\%$, $e_2 = 14.7$ μJ, $a_2 = 58.7\%$, $e_2 = 45.8$ μJ, $a_3 = 26.5\%$ and $-\Delta A_1^{ms}(E \rightarrow \infty)/A = 0.923$. Fitting the vinyl$_A$-RCs with the same set of parameters gives $Y_{IC} = 1 - Y = (24.4 \pm 1\%)$ and $-\Delta A_1^{ms}(E \rightarrow \infty)/A = 0.707$.

version. This ground state recovery process is much more efficient in vinyl$_A$-RCs with its slow charge separation than in the native RCs, because in this case $^1P^*$ is exposed to this process during a much longer period of time. According to Fig. 3 the magnitude of the ms-signal at saturation is $\Delta A_1^{ms}(E \rightarrow \infty)/A = -0.923$ for wild-type RCs. Having determined $\gamma_f = 1 \pm 2\%$ in ns-measurements according to [28] and using $Y_Q \geq 98\%$ [29] and $Y_{IC} \approx 0.2\%$ [35], this allows to determine $\varepsilon_r = -0.95 \pm 0.02$ at 90 K from Eq. 4.

Repetitive pulse saturation experiments shown in Fig. 4 have been carried out at high saturation with average excitation energies of $E = 218$ μJ (wild-type) and 234 μJ (vinyl$_A$-RCs) corresponding to $S = 0.998 \pm 0.0003$ and $S = 0.98 + 0.002/-0.004$, respectively (see Fig. 3). For wild-type RCs we see that steady-state conditions are attained after the very first excitation pulse, which is indicative of a high quantum yield Y_Q. Fitting the data we obtain $\Delta A_\infty^{ms}/A = -0.93 \pm 0.02$ which is identical with the saturation value after single pulse excitation and which according to Eq. 3 gives an alternative assay to $\varepsilon_r = -0.94 \pm 0.02$. Our values for ε_r are larger than the value of -0.88 reported in the literature at 865 nm at 290 K [36]. This difference may be due to the sharpening and the increase of the 890 nm absorption band at low temperatures. In addition we have explicitly accounted for small losses of Q_A, while in [36] the Q_A content was assumed to be 100%.

The repetitive pulse saturation experiment in vinyl$_A$-RCs shows that the steady-state condition is not achieved as quickly as in wild-type RCs. Several pulses are necessary to obtain maximal accumulation of the Q_A-containing RCs in the $P^+Q_A^-$ state. The details of this accumulation process during the first pulses can be used to obtain the yield of B-branch charge separation independent of any ns-data and

will be published elsewhere. Here we refer to ΔA_∞^{ms} values determined after more than 5 pulses. We measure $\Delta A_\infty^{ms} = -0.185$ yielding $\beta = 87.4\%$. Together with $\alpha = 23.6\%$ obtained from the same sample [15], we obtain from Eq. 5 a Q_A content of $1-\gamma_f = (92 \pm 2)\%$ for this sample. This high value shows that the modification of the RCs by introducing vinyl-bacteriochlorophyll under harsh thermal conditions does not seem to deteriorate the Q_A binding ability of the RCs. The small fraction of Q_A-free RCs can only account for part of the nanosecond signal of Fig. 1, which therefore mainly reflects formation of $P^+H_B^-$. From Eq. 2 we get the quantum yield for B-branch charge separation of $Y_B = (12.5 \pm 2)\%$ at 90 K [15].

From Fig. 3 a saturation value $\Delta A_1^{ms}(E \rightarrow \infty)/A = -0.707 \pm 0.02$ was determined for vinyl$_A$-RCs, which may serve as a consistency check when comparing with its theoretical value according to Eq. 4. Inserting all our results we obtain perfect agreement within the error of the measurement.

We want to emphasize the importance of determination of γ_f for an unambiguous proof of B-branch charge separation and for its quantitative determination. The knowledge of γ_f is basic also for quantification of any other kind of loss mechanisms leading to transients in the nanosecond to microsecond regime, which could be mixed up with signals from Q-free RCs. For example, there is evidence that in RCs with B_A substituted by Ni-bacteriochlorophyll fast recombination of $P^+B_A^-$ leads to significant yields of $^3P^*$ even in presence of Q_A [37].

3.1. Conclusions

We have been able to determine the Q_A content of a RC preparation with an accuracy of 2%. Since only the Q_A-containing fraction of RCs can be accumulated in the state $P^+Q_A^-$ after multiple actinic excitation this Q_A content can be derived from the millisecond ground state bleaching at saturating conditions. Knowledge of the Q_A content is essential for discriminating nanosecond transients of $P^+H_A^-$ in Q_A-free RCs from other transients originating from intermediates, which deviate from the standard charge separation sequence along the A-branch. In particular, such measurements are imperative for proving and quantitatively determining B-branch charge separation. This method has been applied to RCs which were deliberately modified to sustain a long lifetime of $^1P^*$ by exchanging the native bacteriochlorophyll against 3-vinyl-13^2-OH-bacteriochlorophyll having a higher redox-potential and which

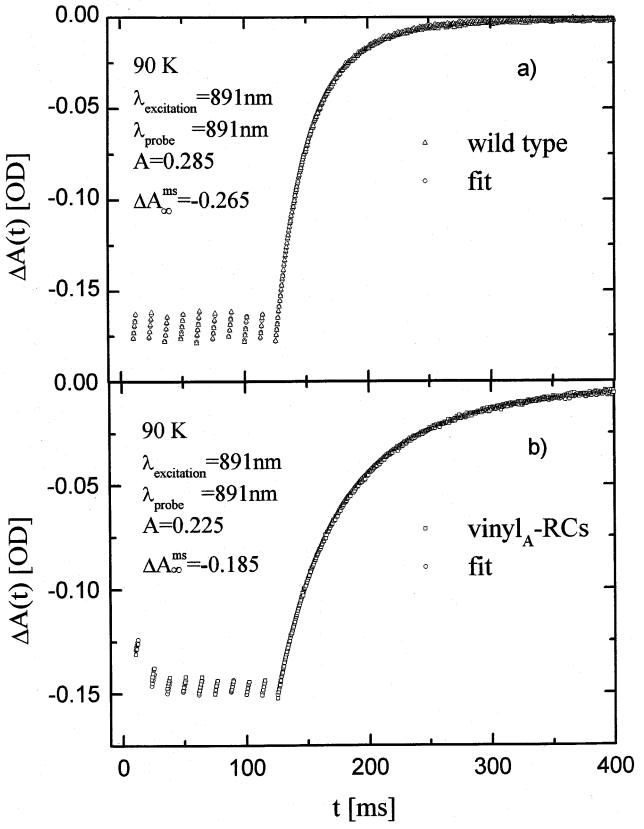

Fig. 4. Millisecond bleaching of the ground state absorption during repetitive saturating excitation: (a) wild-type RCs, (b) vinyl$_A$-RCs. The data points up to 10 ms after each pulse are blanked out making sure signal spikes resulting from stray light of the saturating excitation pulses have decayed completely. The initial value ΔA_∞^{ms} can be extrapolated by fitting the absorption change between each pair of pulses to $\Delta A(t) = \Delta A_\infty^{ms} \sum_{i=1}^{3} a_i \exp(-t/\tau_i)$ based on the following decay characteristics:

Wild type		Vinyl$_a$-RCs	
τ_i	a_i	τ_i	a_i
20.1 ms	57.2%	28.4 ms	38.5%
44.3 ms	42.1%	78.7 ms	60.1%
3396 ms	0.7%	3396 ms	1.5%

which were obtained from fitting the absorption recovery under low stray light conditions after single pulse excitation. Such a dispersive behavior is typical at low temperatures [38] and is attributed to the influence of different protein conformational states.

shows B-branch charge separation [15]. Here we show that in this sample (8 ± 2)% of the RCs had lost Q_A and were responsible for 35% of the detected nanosecond transient. Having once obtained the Q_A content we will be able to analyse a whole temperature-dependent set of nanosecond data and extract the thermal behavior of the B-branch charge separation rate. Such information promises access to the physical origin of unidirectional charge separation [15].

Acknowledgements

This work was supported by the Deutsche Forschungsgemeinschaft (SFB 143).

References

[1] J. Deisenhofer, O. Epp, K. Miki, R. Huber, H. Michel, J. Mol. Biol. 180 (1984) 385–398.
[2] J.P. Allen, G. Feher, T.O. Yeates, D.C. Rees, J. Deisenhofer, H. Michel, R. Huber, Proc. Natl. Acad. Sci. USA 83 (1986) 8589–8593.
[3] C.-H. Chang, D. Tiede, J. Tang, U. Smith, J.R. Norris, M. Schiffer, FEBS Lett. 205 (1986) 82–86.
[4] O. El Kabbani, C.H. Chang, D. Tiede, J.R. Norris, M. Schiffer, Biochemistry 30 (1991) 5361–5369.
[5] U. Ermler, G. Fritsch, S.K. Buchanan, H. Michel, Structure 2 (1994) 925–936.
[6] E.C. Kellogg, S. Kolaczkowski, M.R. Wasielewski, D.M. Tiede, Photosynth. Res. 22 (1989) 47–59.
[7] M. Bixon, J. Jortner, M.E. Michel-Beyerle, A. Ogrodnik, Biochim. Biophys. Acta 977 (1989) 273–286.
[8] W. Aumeier, U. Eberl, A. Ogrodnik, M. Volk, G. Scheidel, R. Feick, M. Plato, M.E. Michel-Beyerle, in: M. Baltscheffsky (Ed.), Current Research in Photosynthesis, vol. I, Kluwer Academic, Amsterdam, 1990, pp. 133–136.
[9] B.A. Heller, D. Holten, C. Kirmaier, Science 269 (1995) 940–945.
[10] J.R. Norris, J. Deisenhofer (Eds.), The Photosynthetic Reaction Center, Academic Press, New York, 1993.
[11] R.E. Blankenship, M.T. Madigan, C.E. Bauer (Eds.), Anoxygenic Photosynthetic Bacteria, Kluwer, Netherlands, 1995.
[12] M.E. Michel-Beyerle (Ed.), Reaction Centers of Photosynthetic Bacteria, Springer, Berlin, 1996.
[13] J.D. McElroy, D.C. Mauzerall, G. Feher, Biochim. Biophys. Acta 333 (1974) 261.
[14] G. Hartwich, G. Bieser, T. Langenbacher, P. Müller, M. Richter, A. Ogrodnik, H. Scheer, M.E. Michel-Beyerle, Biophys. J. 71 (1997) A8, E5.
[15] M.E. Michel-Beyerle, G. Hartwich, M. Richter, A. Ogrodnik, H. Scheer, M. Bixon, J. Jortner, submitted.
[16] E.C. Kellogg, S. Kolaczkowski, M.R. Wasielewski, D.M. Tiede, Photosynth. Res. 22 (1989) 47–59.
[17] C.C. Schenck, R.E. Blankenship, W.W. Parson, Biochim. Biophys. Acta 680 (1982) 44–59.
[18] D.E. Budil, S.V. Kolaczkowski, J.R. Norris, in: J. Biggens (Ed.), Progress in Photosynthesis Research, vol. I, 1, Martinus Nijhoff, Dordrecht, 1987, pp. 25–26.
[19] A. Ogrodnik, M. Volk, R. Letterer, R. Feick, M.E. Michel-Beyerle, Biochim. Biophys. Acta 936 (1988) 361–371.
[20] C.E.D. Chidsey, C. Kirmaier, D. Holten, S.G. Boxer, Biochim. Biophys. Acta 766 (1984) 424–437.
[21] A.J. Hoff, Q. Rev. Biophys. 14 (1981) 599–665.
[22] M. Volk, A. Ogrodnik, M.E. Michel-Beyerle, in: R.E. Blankenship, M.T. Madigan, C.E. Bauer (Eds.), Anoxygenic Photosynthetic Bacteria, Kluwer, Netherlands, 1995, pp. 595–626.
[23] R.J. Cogdell, T.G. Monger, W.W. Parson, Biochim. Biophys. Acta 408 (1975) 189–199.
[24] C.C. Schenck, P. Mathis, M. Lutz, Photochem. Photobiol. 39 (1984) 407–417.
[25] R.J. Cogdell, H.A. Frank, Biochim. Biophys. Acta 895 (1987) 63–79.
[26] H.A. Frank, V. Chynwat, G. Hartwich, M. Meyer, I. Katheder, H. Scheer, Photosynth. Res. 37 (1993) 193–203.
[27] H.A. Frank, V. Chynwat, A. Posteraro, G. Hartwich, I. Simonin, H. Scheer, Photosynth. Res. 64 (1996) 823–831.
[28] M. Volk, G. Aumeier, T. Häberle, A. Ogrodnik, R. Feick, M.E. Michel-Beyerle, Biochim. Biophys. Acta 1102 (1992) 253–259.
[29] C.A. Wraight, R.K. Clayton, Biochim. Biophys. Acta 333 (1974) 246–260.
[30] H.M. Cho, L.J. Mancino, R.E. Blankenship, Biochim. Biophys. Acta 45 (1984) 455–461.
[31] G. Feher, M.Y. Okamura, in: R.K. Clayton, W.R. Sistrom (Eds.), The Photosynthetic Bacteria, Plenum, New York, 1978, pp. 349–386.
[32] A. Struck, H. Scheer, FEBS Lett. 261 (1990) 385–388.
[33] H. Scheer, G. Hartwich, in: R.E. Blankenship, M.T. Madigan, C.E. Bauer (Eds.), Anoxygenic Photosynthetic Bacteria, Kluwer, Netherlands, 1995, pp. 649–664.
[34] G. Hartwich, H. Scheer, V. Aust, A. Angerhofer, Biochim. Biophys. Acta 1230 (1995) 97–113.
[35] P. Müller, G. Bieser, G. Hartwich, T. Langenbacher, H. Lossau, A. Ogrodnik, M.E. Michel-Beyerle, Ber. Bunsenges. Phys. Chem. 100 (1996) 1967–1973.
[36] S.C. Straley, W.W. Parson, D.C. Mauzerall, R.K. Clayton, Biochim. Biophys. Acta 305 (1973) 597–609.
[37] T. Häberle, H. Lossau, M. Friese, G. Hartwich, A. Ogrodnik, H. Scheer, M.E. Michel-Beyerle, in: M.E. Michel-Beyerle (Ed.), The Photosynthetic Reaction Center, Springer, 1996, pp. 239–254.
[38] D. Kleinfeld, M.Y. Okamura, G. Feher, Biochemistry 23 (1984) 5780–5786.